

Einstein-de Haas Effect in Dipolar Bose-Einstein Condensates

Yuki Kawaguchi¹, Hiroki Saito¹, and Masahito Ueda^{1,2}

¹*Department of Physics, Tokyo Institute of Technology,
2-12-1 Ookayama, Meguro-ku, Tokyo 152-8551, Japan*

²*ERATO, Japan Science and Technology Corporation (JST), Saitama 332-0012, Japan*

(Dated: January 27, 2019)

General properties of the order parameter for a dipolar spinor Bose-Einstein condensate are discussed based on symmetries of interactions. An initially spin-polarized dipolar condensate is shown to dynamically generate a non-singular vortex via spin-orbit interactions – a phenomenon reminiscent of the Einstein-de Haas effect in ferromagnets.

PACS numbers: 03.75.Mn,03.75.Nt,03.75.Kk,03.75.Lm

Realization of a Bose-Einstein condensate (BEC) of ^{52}Cr [1, 2] marks a major development in degenerate quantum gases in that the interparticle interaction via magnetic dipoles is much larger than those in the other spinor BECs of alkali atoms. The long-range nature and anisotropy of the dipolar interaction pose challenging questions concerning the stability and superfluidity of the BEC [3, 4, 5, 6, 7, 8, 9, 10]. The ground state of the ^{52}Cr atom has a total electronic spin of three and a nuclear spin of zero, and therefore the ^{52}Cr BEC has seven internal degrees of freedom. The interplay between dipolar and spinor interactions makes the order parameter of this system highly non-trivial [11, 12, 13]. Moreover, the dipole interaction couples the spin and orbital angular momenta so that an initial magnetization of the system causes the gas to rotate mechanically (Einstein-de Haas effect [14]) or, conversely, a solid-body rotation of the system leads to its magnetization (Barnett effect [15]).

The aim of this Letter is to investigate the Einstein-de Haas and the Barnett effects in a spin-3 BEC system. We discuss the symmetry of the order parameter of a dipolar spinor BEC, and study dynamic formation of spin textures using numerical simulations of the seven-component nonlocal mean-field theory, which takes into account short-range (van der Waals) interactions and magnetic dipole-dipole interactions subject to a trapping potential and an external magnetic field.

Let us first investigate general symmetry properties of the order parameter by discussing two fundamental symmetries of the dipolar interaction between magnetic dipole moments $\boldsymbol{\mu}_1 = g\mu_B \hat{\mathbf{s}}_1$ and $\boldsymbol{\mu}_2 = g\mu_B \hat{\mathbf{s}}_2$, where g is the electron g -factor, μ_B is the Bohr magneton, and $\hat{\mathbf{s}}_1$ and $\hat{\mathbf{s}}_2$ are the spin operators. The interaction between the magnetic dipoles located at \mathbf{r}_1 and \mathbf{r}_2 is described by

$$\hat{v}_{dd}(\mathbf{r}_{12}) = c_{dd} \frac{(\hat{\mathbf{s}}_1 \cdot \hat{\mathbf{s}}_2) - 3(\hat{\mathbf{s}}_1 \cdot \mathbf{e}_{12})(\hat{\mathbf{s}}_2 \cdot \mathbf{e}_{12})}{r_{12}^3}, \quad (1)$$

where $\mathbf{r}_{12} \equiv \mathbf{r}_1 - \mathbf{r}_2$, $\mathbf{e}_{12} \equiv \mathbf{r}_{12}/r_{12}$, and $c_{dd} = \mu_0(g\mu_B)^2/4\pi$ with μ_0 being the magnetic permeability of vacuum. The dipole interaction is invariant under simultaneous rotation in spin and coordinate spaces about an arbitrary axis, say the z -axis, so that the projected

total angular momentum operator $\hat{S}_z + \hat{L}_z$ on that axis commutes with \hat{v}_{dd} , where $\hat{\mathbf{S}} = \hat{\mathbf{s}}_1 + \hat{\mathbf{s}}_2$ is the total spin operator and $\hat{\mathbf{L}}$ is the relative orbital angular momentum operator. The other symmetry of the dipolar interaction is the invariance under the transformation $\mathbf{P}_z e^{-i\pi\hat{S}_z}$, where $\mathbf{P}_z : (x, y, z) \rightarrow (x, y, -z)$ and $e^{-i\pi\hat{S}_z} : (\hat{S}_x, \hat{S}_y, \hat{S}_z) \rightarrow (-\hat{S}_x, -\hat{S}_y, \hat{S}_z)$. Thus, the eigenvalues of the following operators are conserved by the dipole interaction:

$$\hat{S}_z + \hat{L}_z \quad \text{and} \quad \mathbf{P}_z e^{-i\pi\hat{S}_z}. \quad (2)$$

A crucial observation here is that these operators also commute with the short-range interactions. Thus if the confining potential is axisymmetric, the simultaneous eigenfunctions of the two operators (2) can serve to classify the two-body wave function.

Constructing a many-body wave function by directly applying these symmetry considerations is quite complicated since the system has many degrees of freedom. However, insight for substantial simplification can be gained by considering the case of a ferromagnet in which dipole moments are localized at lattice sites and thus the degrees of freedom of the system are reduced to the center-of-mass motion and the solid-body rotation around it. Consequently, spin relaxation of the system leads to a solid-body rotation of the ferromagnet – an effect known as the Einstein-de Haas effect [14]. Analogous considerations can be applied to a BEC because almost all atoms occupy a single-particle state, and therefore, the degrees of freedom of the system can be represented by those of the order parameter. We may thus expect the Einstein-de Haas effect to emerge in the dipolar spinor BEC system.

In general, the order parameter of a BEC can be defined as the eigenfunction corresponding to the macroscopic eigenvalue of the reduced single-particle density operator. Let the order parameter be denoted as $\psi_\alpha(\mathbf{r})$ whose norm is assumed to be N , the number of condensate atoms. Here, α represents the magnetic sublevel of atoms. It follows from the above symmetry considerations of the dipolar interaction that the order parameter of a dipolar spinor BEC in an axisymmetric system can

be classified by the eigenvalues of the operators $s^z + l^z$ and $P_z \exp(-i\pi s^z)$ corresponding to the operators (2), where s^z is the z component of the spin matrix and $l^z \equiv -i(\partial/\partial\phi)$. The simultaneous eigenstate of $s^z + l^z$ and $P_z \exp(-i\pi s^z)$ with eigenvalues J and p , respectively, is given by

$$\psi_\alpha(r, \phi, z, t) = e^{i(J-\alpha)\phi} \eta_{\alpha J p}(r, z, t), \quad (3)$$

where J is an integer and $\eta_{\alpha J p}$ is a complex eigenfunction of P_z satisfying $P_z \eta_{\alpha J p} = p(-1)^\alpha \eta_{\alpha J p}$ with $p = \pm 1$. The key point in Eq. (3) is that the spin-dependent phase factor appears, since the dipolar interaction couples the spin with the orbital angular momentum.

We now discuss dynamic formation of spin textures in a dipolar BEC. The order parameter obeys the following set of the nonlocal Gross-Pitaevskii equations:

$$\begin{aligned} i\hbar \frac{d\psi_\alpha(\mathbf{r})}{dt} = & \left[-\frac{\hbar^2 \nabla^2}{2M} + g\mu_B B_{\text{ext}} \alpha + U_{\text{trap}}(\mathbf{r}) \right] \psi_\alpha(\mathbf{r}) \\ & + \sum_{\beta \alpha' \beta'} \sum_{S=0}^{2s} g_S \langle \alpha \beta | \mathcal{P}_S | \alpha' \beta' \rangle \psi_\beta^*(\mathbf{r}) \psi_{\alpha'}(\mathbf{r}) \psi_{\beta'}(\mathbf{r}) \\ & + \sum_{\mu=x,y,z} \sum_{\beta} B_{\text{eff}}^\mu(\mathbf{r}) (g\mu_B s_{\alpha\beta}^\mu) \psi_\beta(\mathbf{r}), \end{aligned} \quad (4)$$

where M is the atomic mass, B_{ext} is the external magnetic field in the z direction, and $U_{\text{trap}}(\mathbf{r})$ is the trapping potential. Here, we assume an optical trap so that all spin components experience the same trapping potential. The second line in Eq. (4) represents the short-range interaction, where the strength of the interaction is characterized by the s -wave scattering length a_S for a total spin S of a pair of atoms with spin s as $g_S = 4\pi\hbar^2 a_S / M$. The operator \mathcal{P}_S projects the wave function into the Hilbert space with a total spin S and is expressed in terms of the Clebsch-Gordan coefficients $\langle s\alpha s\beta | S M_S \rangle$ as $\langle \alpha \beta | \mathcal{P}_S | \alpha' \beta' \rangle = \sum_{M_S=-S}^S \langle s\alpha s\beta | S M_S \rangle \langle S M_S | s\alpha' s\beta' \rangle$ [16].

The last line in Eq. (4) represents the dipole-dipole interaction, where $s^{x,y,z}$ are the spin matrices, and

$$\begin{aligned} B_{\text{eff}}^\mu(\mathbf{r}) \equiv & \frac{c_{\text{dd}}}{g\mu_B} \sum_\nu \int d\mathbf{r}' \frac{\delta_{\mu\nu} - 3e^\mu e^\nu}{|\mathbf{r} - \mathbf{r}'|^3} \\ & \sum_{\alpha' \beta'} \psi_{\alpha'}^*(\mathbf{r}') s_{\alpha' \beta'}^\nu \psi_{\beta'}(\mathbf{r}') \end{aligned} \quad (5)$$

is an effective magnetic field at \mathbf{r} produced by the surrounding magnetic dipoles, with $\mathbf{e} \equiv (\mathbf{r} - \mathbf{r}')/|\mathbf{r} - \mathbf{r}'|$. Calculating the time derivative of $S^\mu(\mathbf{r}) = \sum_{\alpha\beta} \psi_\alpha^*(\mathbf{r}) s_{\alpha\beta}^\mu \psi_\beta(\mathbf{r})$, one finds that, apart from the spinor interactions, $\mathbf{S}(\mathbf{r})$ behaves like a classical spin which undergoes Larmor precession around the effective local magnetic field $\mathbf{B}_{\text{eff}}(\mathbf{r}) + B_{\text{ext}} \hat{z}$. Hence, the spin flip occurs in the region where $B_{\text{eff}}^{x,y}(\mathbf{r}) \neq 0$. In a homogeneous infinite system, the effective field is completely canceled out for a polarized BEC, and the spin flip does not

occur. Therefore, the Einstein-de Haas effect in an initially fully spin-polarized BEC is unique to non-uniform systems.

We study the spin dynamics of the Einstein-de Haas effect in an experimentally realized spin-3 ^{52}Cr BEC system. We consider a situation in which a stable spin-polarized BEC in the lowest spin sublevel $\alpha = -3$ is produced in a strong magnetic field as in the experiments of Refs. [1, 2], and then the magnetic field is suddenly decreased to B_{ext} . The initial state is calculated by the imaginary-time propagation method in the subspace of $\psi_{-3}(\mathbf{r})$. We have performed three-dimensional simulations of Eq. (4) with seven spin components by using the Crank-Nicholson method. The scattering lengths of ^{52}Cr are reported to be $a_6 = 112$, $a_4 = 58$, and $a_2 = -7$ in units of the Bohr radius [17]. The value of a_0 is unknown and we estimate it by using the van der Waals coefficient C_6 given in Ref. [17] as $a_0 \sim (C_6 M/m_e)^{1/4} = 91$, where m_e is the electron mass. Since we are interested in spin dynamics from a fully spin-polarized state, the short-range interaction is dominated by a_6 and a_4 [18].

We assume $N = 10^5$ atoms trapped in an axisymmetric potential $U_{\text{trap}}(\mathbf{r}) = (1/2)M\omega^2(r^2 + z^2/\lambda^4)$ with $\omega = 2\pi \times 820$ Hz. The typical ratio of the dipolar interaction to the short-range interaction is $s^2 c_{\text{dd}}/g_6 \simeq 0.03$ with $s = 3$. In a spherical trap, the number density at the trap center is $n \simeq 7 \times 10^{20} \text{ m}^{-3}$ and the dipole-dipole interaction energy $s^2 c_{\text{dd}} n$ becomes the same order of magnitude as the Zeeman energy for $B_{\text{ext}} \simeq 0.1$ mG. Hence, the spin-flip rate becomes significant for $|B_{\text{ext}}| \lesssim 1$ mG. In the following, we first consider $B_{\text{ext}} = 0$ and $\lambda = 1$, and then discuss the effects of the external magnetic field and the trap geometry on spin dynamics.

Figure 1 shows the results for $B_{\text{ext}} = 0$ and $\lambda = 1$. In Fig. 1(a), we plot the population of each spin state $N_\alpha/N \equiv \int d\mathbf{r} |\psi_\alpha|^2 / N$ as a function of ωt . We see that N_{-2}/N first increases rapidly and then the components with $\alpha \geq -1$ grow. Figures 1(b), (c), and (d) show the three-dimensional plots of ψ_{-3} , ψ_{-2} , and ψ_{-1} at $\omega t = 2$, respectively, where the values of $|\psi_\alpha|^2$ are scaled by N/a_{ho}^3 with a_{ho} being the harmonic oscillator length $\sqrt{\hbar/2M\omega}$. The order parameters indeed show the symmetries discussed in Eq. (3): ψ_{-2} has a phase factor $e^{-i\phi}$ and the node plane at $z = 0$, and ψ_{-1} has a phase factor $e^{-2i\phi}$ and reflection symmetry with respect to the $z = 0$ plane. The other spin components have double-ring shapes similar to Fig. 1(d) and their phase relationship satisfies Eq. (3) with $J = -3$ and $p = -1$. After $\omega t = 5$ the system develops a complicated structure of the spinor order parameter.

The effective magnetic field (5) at $\omega t = 0$ and the spin vector $\mathbf{S}(\mathbf{r})$ at $\omega t = 2$ are plotted in Fig. 2. The whirling patterns of the spin texture in Figs. 2(b) and (c) are due to the Larmor precession around the local magnetic field shown in Fig. 2(a). Since the local magnetic field points outward for $z > 0$ and inward for $z < 0$, the directions of

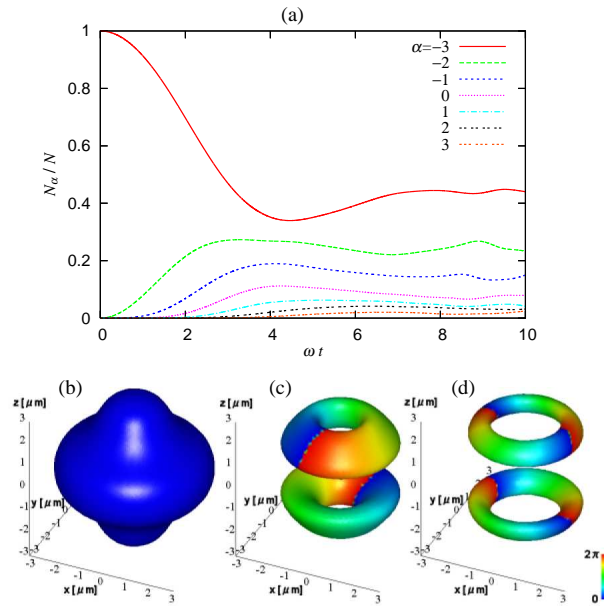


FIG. 1: (Color) (a) Relative population $N_\alpha/N = \int d\mathbf{r} |\psi_\alpha|^2/N$ of each magnetic sublevel α versus ωt for $B_{\text{ext}} = 0$ and $\lambda = 1$. (b)-(d) Isopycnic surfaces of (b) ψ_{-3} , (c) ψ_{-2} , and (d) ψ_{-1} at $\omega t = 2$, where $|\psi_\alpha|^2 a_{\text{ho}}^3/N = 0.0001$ for (b) and (c) and 5×10^{-5} for (d). The color on the surface represents the phase of the order parameter (see the right gauge).

the whirlpools in Figs. 2(b) and (c) are opposite. Topological spin textures in spinor BECs have been observed in a spin-1/2 system [19] and in a spin-1 system [20]. We note that the spin textures in Figs. 2(b) and (c) are generated spontaneously due to the intrinsic dipole interaction in contrast to those in Refs. [19, 20] which are generated by external forces.

When the external magnetic field B_{ext} is applied in the positive z direction and is much stronger than the dipole field, the spin angular momentum should be conserved because of energy conservation, and spin flip is suppressed. When $B_{\text{ext}} < 0$, spin flip can occur by converting the Zeeman energy to kinetic energy. These behaviors are demonstrated in Fig. 3(a), in which the time evolution of N_{-2}/N for $B_{\text{ext}} = \pm 1$ mG is plotted. Figures 3(b) and (c) show cross sections of $|\psi_{-2}|^2 a_{\text{ho}}^3/N$ for $B_{\text{ext}} = \pm 1$ mG at $\omega t = 8$ and $\lambda = 1$. When $B_{\text{ext}} > 0$, ψ_{-2} oscillates in time between the structure of Fig. 1(c) and that of Fig. 3(b). These structures are derived by the symmetry of the dipole interaction, which is expressed in terms of the rank-2 spherical harmonics Y_{2m} . The dipole field produced by an approximately spherical distribution of $\psi_{-3} \sim Y_{00}(\mathbf{r})$ induces a $Y_{2-1}(\mathbf{r})$ term in ψ_{-2} (Fig. 1(c)) which, in turn, affects itself and induces a linear combination of $Y_{2-1}(\mathbf{r})$ and $Y_{4-1}(\mathbf{r})$, resulting in Fig. 3(b). Therefore, the structure in Fig. 3(b) manifests itself as a secondary effect of the dipole-dipole interaction. In the case of $B_{\text{ext}} = -1$ mG, a similar structure as in Fig. 3(b)

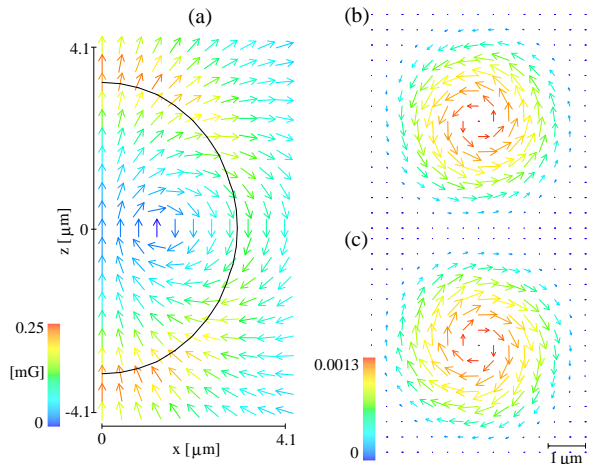


FIG. 2: (Color) (a) Dipole field at $t = 0$ for $\lambda = 1$. The solid curve shows isopycnic curve at $|\psi_{-3}|^2 a_{\text{ho}}^3/N = 0.0001$. The color of the arrows denotes the magnitude of the field. (b)(c) Spin configurations on the (b) $z = 2 \mu\text{m}$ plane and (c) $z = -2 \mu\text{m}$ plane at $\omega t = 2$ for $B_{\text{ext}} = 0$ and $\lambda = 0$. The length of the arrow represents the magnitude of the spin vector projected on the xy -plane and the color shows $|S| a_{\text{ho}}^3/N$. Note that spins tilt in a direction perpendicular to $\mathbf{B}_{\text{eff}}(\mathbf{r})$.

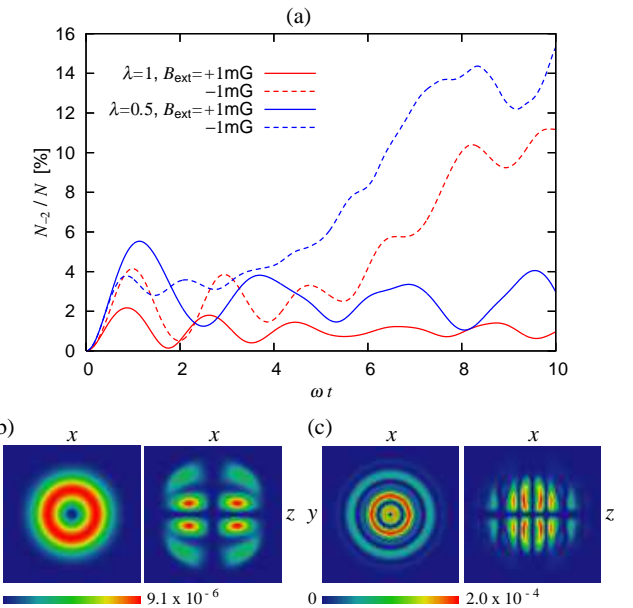


FIG. 3: (Color) (a) Population of $\alpha = -2$ sublevel versus ωt for $B_{\text{ext}} = \pm 1$ mG and $\lambda = 1$ and 0.5. (b)(c) Cross sections of $|\psi_{-2}|^2 a_{\text{ho}}^3/N$ with $\lambda = 1$ at $\omega t = 8$ for (b) $B_{\text{ext}} = 1$ mG and (c) -1 mG. The cross sections are at $z = 0.7 \mu\text{m}$ (left) and $y = 0 \mu\text{m}$ (right). The size of each panel is $8.2 \times 8.2 \mu\text{m}$.

appears when $\omega t \lesssim 4$. However, as time advances, the domain structure develops as shown in Fig. 3(c). The domain size becomes smaller as the value of $|B_{\text{ext}}|$ increases.

Finally, we discuss the geometry dependence of the dy-

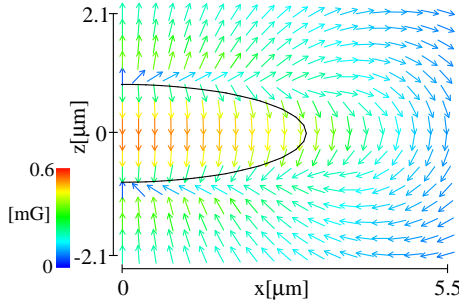


FIG. 4: (Color) Dipole field at $t = 0$ for $\lambda = 0.5$. The solid curve shows an isopycnic curve at $|\psi_{-3}|^2 a_{ho}^3 / N = 0.0005$. Note that the sign of $B_{\text{eff}}^z(\mathbf{r})$ in the condensate is opposite to that in Fig. 2(a).

namics. Figure 4 shows the dipole field $\mathbf{B}_{\text{eff}}(\mathbf{r})$ at $t = 0$ for $\lambda = 0.5$. Compared with Fig. 2(a), the z component of the effective magnetic field is inverted around the center of the condensate. The transfer of atoms from the spin sublevel $\alpha = -3$ to $\alpha \geq -2$ is due to the Larmor precession caused by B_{eff}^{xy} , and it occurs most efficiently at the place where the local magnetic field in the z direction $B_{\text{eff}}^z + B_{\text{ext}}$ vanishes. The sign of such optimized B_{ext} for spherical traps is opposite to that for pancake-shaped traps, as can be inferred from Fig. 2(a) and Fig. 4. This fact is indeed reflected in Fig. 3(a) as the difference in the field dependence of the initial peaks. Since the z component of the dipole field is positive in most of the condensate when $\lambda = 1$ (Fig. 2(a)), the initial peak in Fig. 3(a) is larger for $B_{\text{ext}} = -1$ mG than for $B_{\text{ext}} = 1$ mG. The relation between the initial peak and B_{ext} is opposite in the case for $\lambda = 0.5$, since the z component of the dipole field is mostly negative in the condensate (Fig. 4). In the case of a cigar-shaped BEC, qualitative behavior is the same as in the spherical trap.

In conclusion, we have shown that the Einstein-de Haas effect occurs in dipolar spinor Bose-Einstein condensates and that a non-singular vortex appears from an initially spin-polarized condensate. In a low magnetic field (~ 1 mG) the fraction of the spin-flipped atoms ($\sim 5\%$) is large enough to be observed in Stern-Gerlach experiments. The spin-relaxation processes produce various vortex structures, depending on the external magnetic field.

This work was supported by Grant-in-Aids for Scientific Research (Grant No. 17740263, No. 17071005, and No. 15340129) and by a 21st Century COE program at Tokyo Tech “Nanometer-Scale Quantum Physics” from the Ministry of Education, Culture, Sports, Science and Technology of Japan. YK acknowledges support by a Fel-

lowship Program of the Japan Society for Promotion of Science (Project No. 160648). MU acknowledges support by a CREST program of the JST.

Note added. — Very recently, a preprint [21] appeared which also discusses the Einstein-de Haas effect in a dipolar BEC.

- [1] A. Griesmaier, J. Werner, S. Hensler, J. Stuhler, and T. Pfau, Phys. Rev. Lett. **94**, 160401 (2005).
- [2] J. Stuhler, A. Griesmaier, T. Koch, M. Fattori, T. Pfau, S. Giovanazzi, P. Pedri, and L. Santos, Phys. Rev. Lett. **95**, 150406 (2005).
- [3] L. Santos, G. V. Shlyapnikov, P. Zoller, and M. Lewenstein, Phys. Rev. Lett. **85**, 1791 (2000).
- [4] L. Santos, G. V. Shlyapnikov, and M. Lewenstein, Phys. Rev. Lett. **90**, 250403 (2003).
- [5] K. Góral and L. Santos, Phys. Rev. A **66**, 023613 (2002).
- [6] K. Góral, K. Rzazewski, and T. Pfau, Phys. Rev. A **61**, 051601(R) (2000).
- [7] D. H. J. O’Dell, S. Giovanazzi, and C. Eberlein, Phys. Rev. Lett. **92**, 250401 (2004).
- [8] C. Eberlein, S. Giovanazzi, and D. H. J. O’Dell, Phys. Rev. A **71**, 033618 (2005).
- [9] S. Yi and L. You, Phys. Rev. A **63**, 053607 (2001).
- [10] M. Baranov, L. Dobrek, K. Góral, L. Santos, and M. Lewenstein, Physica Scripta. **T102**, 74 (2002).
- [11] S. Yi, L. You, and H. Pu, Phys. Rev. Lett. **93**, 040403 (2004).
- [12] H. Pu, W. Zhang, and P. Meystre, Phys. Rev. Lett. **87**, 140405 (2001).
- [13] K. Gross, C. P. Search, H. Pu, W. Zhang, and P. Meystre, Phys. Rev. A **66**, 033603 (2002).
- [14] A. Einstein and W. J. de Haas, Verhandl. Deut. Physik Gas **17**, 152 (1915).
- [15] S. J. Barnett, Phys. Rev. **6**, 239 (1915).
- [16] T.-L. Ho, Phys. Rev. Lett. **81**, 742 (1998).
- [17] J. Werner, A. Griesmaier, S. Hensler, J. Stuhler, T. Pfau, A. Simoni, and E. Tiesinga, Phys. Rev. Lett. **94**, 183201 (2005).
- [18] After submission of our paper, we became aware of a reprint by R. B. Diener and T.-L. Ho (cond-mat/0511751). Our choice of $a_0 = 91$ corresponds to the C phase of this reference. We have also investigated the A and B phases in the same reference by taking other values of a_0 and found almost the same spin dynamics as that for $a_0 = 91$.
- [19] M. R. Matthews, B. P. Anderson, P. C. Haljan, D. S. Hall, M. J. Holland, J. E. Williams, C. E. Wieman, and E. A. Cornell, Phys. Rev. Lett. **83**, 3358 (1999).
- [20] A. E. Leanhardt, Y. Shin, D. Kielpinski, D. E. Pritchard, and W. Ketterle, Phys. Rev. Lett. **90**, 140403 (2003).
- [21] L. Santos and T. Pfau, cond-mat/0510634.